Original Article | Thoracic Imaging

eISSN 2005-8330
https://doi.org/10.3348/kjr.2020.0454
Korean J Radiol 2021;22(4):652-662

Korean Journal of Radiology
KJR

Primary Invasive Mucinous Adenocarcinoma of the Lung: Prognostic Value of CT Imaging Features Combined with Clinical Factors

Tingting Wang, MD[1]*, Yang Yang, MD[1]*, Xinyue Liu, MD[2], Jiajun Deng, MD[2], Junqi Wu, MD[2], Likun Hou, MD[3], Chunyan Wu, MD[3], Yunlang She, MD[2], Xiwen Sun, MD, PhD[1], Dong Xie, MD, PhD[2], Chang Chen, MD, PhD[2]

Departments of [1]Radiology, [2]Thoracic Surgery, and [3]Pathology, Shanghai Pulmonary Hospital, Tongji University School of Medicine, Shanghai, China

Objective: To investigate the association between CT imaging features and survival outcomes in patients with primary invasive mucinous adenocarcinoma (IMA).

Materials and Methods: Preoperative CT image findings were consecutively evaluated in 317 patients with resected IMA from January 2011 to December 2015. The association between CT features and long-term survival were assessed by univariate analysis. The independent prognostic factors were identified by the multivariate Cox regression analyses. The survival comparison of IMA patients was investigated using the Kaplan-Meier method and propensity scores. Furthermore, the prognostic impact of CT features was assessed based on different imaging subtypes, and the results were adjusted using the Bonferroni method.

Results: The median follow-up time was 52.8 months; the 5-year disease-free survival (DFS) and overall survival rates of resected IMAs were 68.5% and 77.6%, respectively. The univariate analyses of all IMA patients demonstrated that 15 CT imaging features, in addition to the clinicopathologic characteristics, significantly correlated with the recurrence or death of IMA patients. The multivariable analysis revealed that five of them, including imaging subtype ($p = 0.002$), spiculation ($p < 0.001$), tumor density ($p = 0.008$), air bronchogram ($p < 0.001$), emphysema ($p < 0.001$), and location ($p = 0.029$) were independent prognostic factors. The subgroup analysis demonstrated that pneumonic-type IMA had a significantly worse prognosis than solitary-type IMA. Moreover, for solitary-type IMAs, the most independent CT imaging biomarkers were air bronchogram and emphysema with an adjusted p value less than 0.05; for pneumonic-type IMA, the tumors with mixed consolidation and ground-glass opacity were associated with a longer DFS (adjusted $p = 0.012$).

Conclusion: CT imaging features characteristic of IMA may provide prognostic information and individual risk assessment in addition to the recognized clinical predictors.

Keywords: *Invasive mucinous adenocarcinoma; Computed tomography; Prognosis*

INTRODUCTION

Lung cancer remains the highest contributor to cancer death worldwide despite promising progress in screening, diagnosis, and treatment (1, 2). Lung adenocarcinoma (ADC) is the most common subtype with its proportion over 40%, the incidence and mortality rate of which has kept increasing (3, 4). The classification system of lung ADC, proposed by the International Association for the Study of Lung Cancer, the American Thoracic Society, and the

Received: April 13, 2020 **Revised:** June 29, 2020 **Accepted:** July 2, 2020
This work was supported by Shanghai Municipal Health Commission (2018ZHYL0102, 2019SY072), and Shanghai Pulmonary Hospital Research Fund (FK1941, FK1936).
*These authors contributed equally to this work.
Corresponding author: Chang Chen, MD, PhD, Department of Thoracic Surgery, Shanghai Pulmonary Hospital, Tongji University School of Medicine, Zhengmin Rd. 507, Shanghai 200443, China.
• E-mail: changchenc@tongji.edu.cn

Korean Journal of Radiology
KJR

European Respiratory Society in 2011, provides a widely applicable guide for their clinical management (5). This system considers invasive mucinous adenocarcinoma (IMA), formerly known as mucinous bronchioloalveolar carcinoma, as a variant subtype of invasive ADC. IMA is characterized by invasive columnar or goblet cell patterns with basally located nuclei and abundant intracytoplasmic mucin (6).

IMA has remarkably different molecular, clinicopathological, and radiologic characteristics compared with other subtypes of ADC (7, 8). Meanwhile, limited researches with conflicting results have revealed that the prognosis of IMA is not as well typified as that of non-mucinous ADC (9). Several clinicopathologic factors, such as tumor size and tumor, node, and metastasis (TNM) stage, were reported to be potential biomarkers for worse prognosis in IMA patients (9-11). However, an extremely wide spectrum of tumor behavior in IMA resulted in their survival outcomes not adequately reflected by these recognized prognostic factors in clinical perspective.

Imaging tools, including CT, are well-established modalities routinely used for initial diagnostic staging, guiding treatment-making, and monitoring prognostication of lung cancer in clinical practice (3, 12). Distinct CT findings, including tumor imaging patterns, mixed air-space consolidation, and ground-glass opacity (GGO), air bronchogram, have been reported to be characteristic in IMA patients (13-15). In terms of survival prediction in IMA, few studies suggested that CT manifesting subtype could be an effective indicator (9-11, 14, 16). However, to date, comprehensive clinical or imaging studies on IMA are limited due to the relatively rare histology, and the prognostic utility of more detailed radiologic information that complement the current predictors may need further exploration.

We hypothesized that the use of radiologic features might lead to a better prognostic discrimination of IMA patients. Therefore, in this study, we aimed to investigate the prognostic impact of CT imaging features in patients who received surgical resection of IMA.

MATERIALS AND METHODS

Patients Selection

Our institutional review board approved this retrospective study and waived the informed consent. Altogether, 402 patients diagnosed with IMA, from January 2011 to December 2015, were initially included. Among them, 85 patients were excluded according to the following predefined exclusion criteria: 1) those metastasized from gastrointestinal or other mucinous ADC (n = 12); 2) those who did not receive surgical resection but were diagnosed only through biopsy (n = 16); 3) those who underwent preoperative radiation therapy or chemotherapy (n = 10); 4) those who lack complete clinicopathologic data and follow-up records (n = 25); and 5) those who lack CT images (n = 22). Ultimately, 317 patients were enrolled in this study.

Two pathologists (10 and 20 years of experience in pathological diagnosis of lung cancer, respectively) re-evaluated all histological slides which were formalin-fixed and stained with hematoxylin and eosin and any disagreement was resolved by discussion. According to the 2015 WHO ADC classification, tumor cells having more than 95% of goblet or columnar cell morphologic patterns with abundant intracytoplasmic mucin were recorded as IMA (17). The included patients were reclassified according to the 8th edition of the American Joint Committee on Cancer/Union for International Cancer Control TNM staging system (18). The follow-up protocol of these patients is described in Supplementary Materials 1. Disease-free survival (DFS) was calculated from their surgery date to the time of first lung cancer–related recurrence, or last follow-up. Overall survival (OS) was calculated from the surgery date to that of death or last follow-up.

CT Image Acquisition and Interpretation

All patients underwent thoracic CT examinations before surgery in our institution, and the detailed scanning parameters are shown in Supplementary Materials 2. Two board-certified radiologists (3 and 6 years of experience in thoracic CT imaging diagnosis, respectively) independently interpreted the thin-section CT images using both the lung (width, 1500 Hounsfield unit [HU]; level, -400 HU) and mediastinal (width, 400 HU; level, 40 HU) window setting. The recorded CT findings of all patients were verified by a senior radiologist (30 years of experience in lung cancer diagnosis) and final decisions were reached by discussion. All observers were blinded to the survival outcomes but aware of the target lesion location.

The CT imaging features were evaluated to characterize the lesions and their surroundings. A detailed definition of these CT descriptors and their case examples are provided (Fig. 1, Supplementary Table 1, Supplementary Fig. 1). Solitary-type IMA was defined as a solitary nodule or mass with a defined shape; pneumonic-type IMA was defined

 https://doi.org/10.3348/kjr.2020.0454

as a tumor distributed extensively in the lung lobe (14). Moreover, we manually quantified spiculations as lines extending from the lesion margin into the lung parenchyma without reaching the pleura, and the presence of spiculations was dichotomized according to their median number as few and many (n = 4). The spiculation could be coarse (thicker than 2 mm) or fine (thinner than 2 mm) (19).

Statistical Analysis

The reader agreement was estimated using "irr" package on R programming (version 3.5.3; http://www.R-project.org). The κ index was measured for categorical features, and the Kendall coefficient of concordance for ordinal variables; the intraclass correlation coefficient (ICC) was calculated for continuous variables.

Baseline characteristics were compared using Pearson's chi-squared test or Fisher's exact test for categorical variables, and Student's *t* test for continuous variables. The DFS and OS of patients were evaluated using the Kaplan-Meier method and log-rank test with "survival" package, while the median follow-up time was measured by the reverse Kaplan-Meier method. Further analysis of prognosis in IMA patients was performed using the Cox regression analysis. Variables with $p < 0.05$ in univariable analysis were included in the multivariable Cox regression model with backward stepwise selection. SPSS for Windows,

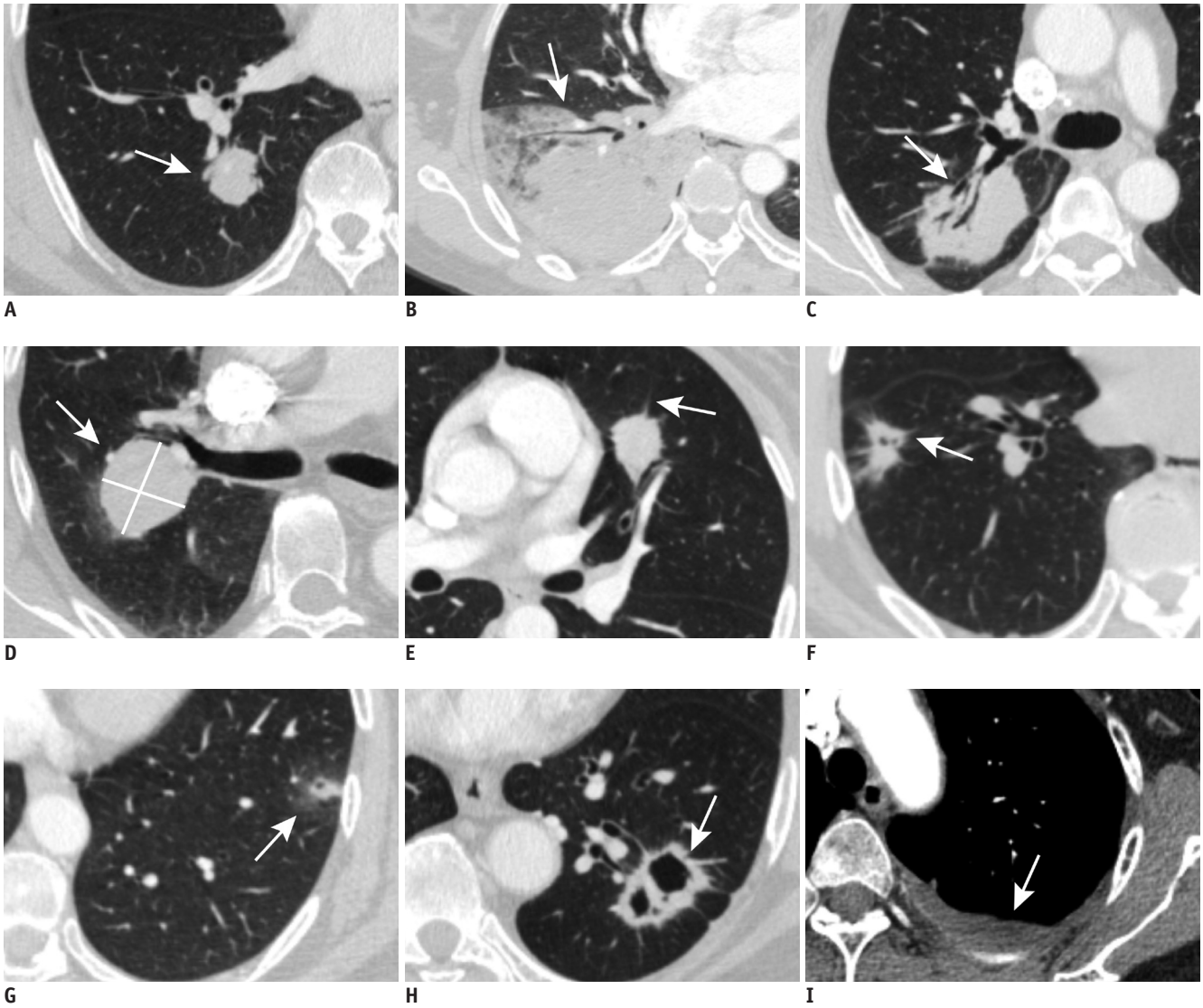

Fig. 1. Illustration of imaging features (arrows) of patients with lung IMA shown on axial CT images (lung window setting: width, -400 HU; level, 1500 HU; mediastinal window setting: width, 400 HU; level, 40 HU).
A. Solitary-type IMA. **B.** Pneumonic-type IMA. **C.** Air bronchogram. **D.** The absence of spiculation. **E.** Few spiculation (n ≤ 4). **F.** Much spiculation (n > 4). **G.** Sub-solid tumor. **H.** Cavitation. **I.** Pleural effusion. HU = Hounsfield unit, IMA = invasive mucinous adenocarcinoma

https://doi.org/10.3348/kjr.2020.0454

Korean Journal of Radiology
KJR

version 20.0 (IBM Corp.) was used for the above statistical analyses. A *p* value lower than 0.05 was statistically significant.

Because solitary-type and pneumonic-type IMAs were recognized to have various tumor heterogeneities, subgroup analyses based on this imaging subtype were performed to compare their prognosis. The results from multiple testing were adjusted using the Bonferroni method (20). Furthermore, a propensity score-matching analysis (4:1) using the "MatchIt" package was performed based on a non-random allocation to minimize the bias caused by sample size difference. Propensity scores were estimated using a logistic model including age, sex, smoking status, surgery type, overall stage, visceral pleural invasion (VPI), and pathologic tumor size.

RESULTS

Reader Agreement

In the imaging observations of this study, the κ index and Kendall coefficient of concordance for categorical features were greater than 0.7 (Supplementary Table 2). The ICC for spiculations was 0.850 (0.878–0.817). All extracted CT features with concordance coefficients > 0.7 were regarded as highly reproducible.

Correlation of Clinicopathologic Features with DFS and OS

The clinicopathologic characteristics of all the cases are summarized in Table 1. In total, we included 317 patients (192 women [60.6%], 125 men [39.4%]; median age, 60 years, age range, 30–82 years) with resected IMA in this study. The mean tumor size in the pathologic specimen was 31.2 mm (standard deviation: 22.3 mm). According to the 8th edition of the TNM staging system, 220 (69.4%) patents were in stage I, 54 (17.0%) in stage II, and 43 (13.6%) in stage III. Among them, the median follow-up time was 52.8 months (range: 8.3–100.8 months), and the 5-year DFS and OS rates were 68.5% and 77.6%, respectively (Fig. 2).

The univariate analyses (Table 1) found that female patients had a longer DFS and OS than male patients ($p = 0.011$ and $p = 0.002$, respectively). With regard to the pathologic predictors, advanced overall stage (both $p < 0.001$), positive VPI ($p = 0.001$ and $p = 0.002$, respectively), and larger tumor size (both $p < 0.001$) were associated with worse prognosis. However, there was no significant correlation between the survival and age, smoking status and surgery types.

Correlation of CT Imaging Features with DFS and OS

The distribution of all interpreted CT imaging features and their association with patients' survival are displayed in Table 2. At baseline, 291 patients (91.8%) had solitary-type IMAs and 26 (8.2%) had pneumonic-type IMAs on CT. The univariable analysis revealed that the patients with pneumonic-type IMAs had a significantly higher risk of recurrence and death than those with solitary-type IMAs, with hazard ratios (HRs) of 4.429 (95% confidence interval

Table 1. The Clinicopathologic Factors Predicting the Prognoses in 317 IMA Patients

Characteristics	IMA (n = 317)	DFS		OS	
		HR (95% CI)	*P*	HR (95% CI)	*P*
Age (years), median (range)	60 (30–82)				
< 60 (ref.) vs. ≥ 60	164 (51.7)/153 (48.3)	1.071 (0.724–1.585)	0.732	1.160 (0.728–1.847)	0.532
Sex					
Female (ref.) vs. male	192 (60.6)/125 (39.4)	1.664 (1.124–2.464)	0.011	2.068 (1.296–3.302)	0.002
Smoking history					
Never (ref.) vs. smoking	214 (67.5)/103 (32.5)	1.399 (0.935–2.092)	0.102	1.256 (0.775–2.036)	0.355
Surgery type					
Sublobar (ref.) vs. lobe	53 (17.7)/261 (82.4)	1.138 (0.667–1.944)	0.635	0.912 (0.499–1.665)	0.764
Overall stage			< 0.001		< 0.001
I (ref.) vs. II	220 (69.4)/54 (17.0)	3.719 (2.273–6.087)	< 0.001	4.610 (2.547–8.345)	< 0.001
I (ref.) vs. III	220 (69.4)/43 (13.6)	8.595 (5.383–13.723)	< 0.001	9.566 (5.467–16.740)	< 0.001
VPI					
Absence (ref.) vs. presence	214 (67.5)/103 (32.5)	1.902 (1.282–2.820)	0.001	2.089 (1.311–3.328)	0.002
Tumor size, mm, mean ± SD	31.2 ± 22.3	1.244 (1.177–1.315)	< 0.001	1.267 (1.194–1.345)	< 0.001

CI = confidence interval, DFS = disease-free survival, HR = hazard ratio, IMA = invasive mucinous adenocarcinoma, OS = overall survival, ref = reference, VPI = visceral pleural invasion

https://doi.org/10.3348/kjr.2020.0454

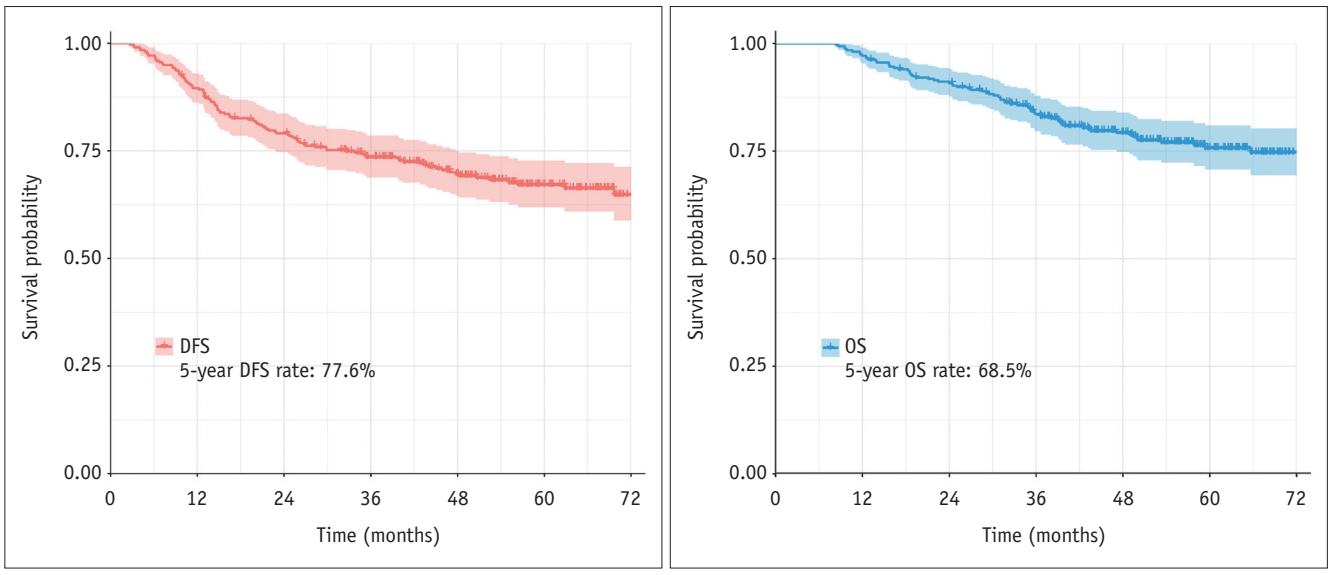

Fig. 2. DFS (A) and OS (B) of patients with primary IMA of the lung. DFS = disease-free survival, OS = overall survival

[CI]: 2.669–7.349, $p < 0.001$) and 5.490 (95% CI: 3.168–9.514, $p < 0.001$), respectively. Other tumor characteristics, including central tumor ($p < 0.001$), much spiculation ($p = 0.001$), pure-solid density ($p < 0.001$), cavitation ($p = 0.006$), and air bronchogram ($p < 0.001$) were frequently found among patients with a worse DFS. The presence of those associated findings, including lymphadenopathy ($p < 0.001$), emphysema ($p < 0.001$), pleural effusion ($p = 0.002$), usual interstitial pneumonia pattern ($p = 0.001$), additional lesions existing in the non-tumor lobe ($p = 0.019$), and obstructive pneumonia ($p = 0.040$) also significantly correlated with a shorter DFS time in IMA patients. Similarly, those aforementioned significant CT imaging features were also associated with OS (Table 2, all $p < 0.05$). In addition, tumors attached to the pleura were significantly associated with poor OS ($p = 0.023$) but not DFS ($p = 0.206$).

Multivariable Analyses of Prognostic Factors

Further analysis of the risk of recurrence and death of IMA was performed using the multivariate Cox proportional hazard regression model (Table 3). After adjusting for all other significant imaging variables, the imaging subtype remained as an independent prognostic factor in IMA patients (HR for DFS, 2.344; 95% CI, 1.131–4.857; $p = 0.002$). Furthermore, the presence of much spiculation ($p < 0.001$), emphysema ($p < 0.001$), the absence of an air bronchogram ($p < 0.001$), and tumors manifesting as pure-solid density ($p = 0.008$), were independent risk predictors for a shorter DFS time. The model for OS prediction indicated that the tumor location ($p = 0.029$), the absence of an air bronchogram ($p = 0.011$), advanced TNM stage ($p < 0.001$), and larger tumor size ($p = 0.019$) were independent factors for an increased risk of death.

Survival Comparison Analysis between the Imaging Subtypes

The clinicopathologic characteristics (Supplementary Table 3) and CT imaging features (Supplementary Table 4) in solitary-type IMA differed from those in the pneumonic-type IMA. As for their prognoses, during the follow-up period, 81 patients with solitary-type IMAs and 19 patients with pneumonic-type IMAs experienced disease relapse, while 54 patients with solitary-type IMAs and 17 patients with pneumonic-type IMAs died after surgical resection. The Kaplan-Meier analyses suggested that pneumonic-type IMAs had significantly higher recurrences and death rates than solitary-type IMAs (both $p < 0.001$) (Fig. 3A). The propensity matching generated a subset consisting of 62 patients with solitary-type (n = 49) and pneumonic-type (n = 13) IMAs among which the clinicopathologic factors were comparable. The matched survival analysis confirmed the worse prognosis of pneumonic-type IMAs ($p < 0.002$) (Fig. 3B).

In the subgroup of solitary-type IMA (Table 4), the multivariate analyses demonstrated that the most important and significantly independent prognostic factors was the presence of an air bronchogram (both adjusted $p = 0.002$),

https://doi.org/10.3348/kjr.2020.0454

Korean Journal of Radiology
KJR

emphysema (adjusted $p = 0.024$ and $p = 0.034$ for DFS and OS, respectively), and the advanced TNM stage (all adjusted $p < 0.001$ for DFS and OS). However, for the subgroup of pneumonic-type IMA (Supplementary Table 5), all described clinicopathological factors and interpreted CT imaging features were not statistically significant in predicting

Table 2. The Univariable Analysis of CT Imaging Features Predicting the Prognosis of 317 IMA Patients

CT Imaging Features	IMA (n = 317)	DFS		OS	
		HR (95% CI)	*P*	HR (95% CI)	*P*
Imaging type					
Solitary-type (ref.) vs. pneumonic-type	291 (91.8)/26 (8.2)	4.429 (2.669–7.349)	< 0.001	5.490 (3.168–9.514)	< 0.001
Location					
Peripheral (ref.) vs. central	283 (89.3)/34 (10.7)	2.606 (1.594–4.259)	< 0.001	3.201 (1.853–5.530)	< 0.001
Tumor lobe					
Left lobe (ref.) vs. right lobe	141 (44.5)/176 (55.5)	1.334 (0.892–1.994)	0.161	1.369 (0.848–2.211)	0.199
Overall shape					
Round (ref.) vs. irregular	202 (63.7)/115 (36.3)	1.358 (0.913–2.021)	0.131	1.202 (0.746–1.934)	0.450
Lobulation			0.830		
Absence (ref.) vs. shallow	114 (36.0)/92 (29.0)	0.859 (0.526–1.403)	0.543	0.760 (0.430–1.343)	0.345
Absence (ref.) vs. deep	114 (36.0)/111 (35.0)	0.949 (0.598–1.507)	0.825	0.731 (0.420–1.272)	0.268
Border					
Clear (ref.) vs. obscure	183 (57.7)/134 (42.3)	1.340 (0.904–1.985)	0.144	1.559 (0.978–2.484)	0.062
Spiculation			< 0.001		0.010
Absence (ref.) vs. few (≤ 4)	155 (48.9)/99 (31.2)	0.679 (0.404–1.143)	0.145	0.482 (0.256–0.907)	0.024
Absence (ref.) vs. much (> 4)	155 (48.9)/63 (19.9)	2.181 (1.399–3.400)	0.001	1.407 (0.823–2.403)	0.212
Spiculation (fine as ref.)					
Fine (ref.) vs. coarse	33 (10.4)/131 (41.3)	1.717 (0.813–3.628)	0.157	2.146 (0.757–6.081)	0.151
Pleural attachment					
Absence (ref.) vs. presence	151 (47.6)/166 (52.4)	1.291 (0.869–1.919)	0.206	1.756 (1.079–2.859)	0.023
Pleural retraction					
Absence (ref.) vs. presence	211 (66.6)/106 (33.4)	1.279 (0.856–1.911)	0.230	1.885 (0.637–1.687)	0.885
Tumor density					
Sub-solid (ref.) vs. pure-solid	62 (19.6)/255 (80.4)	4.391 (1. 923–10.025)	< 0.001	3.392 (1.367–8.420)	0.008
Calcifications					
Absence (ref.) vs. presence	311 (98.1)/6 (1.9)	0.990 (0.244–4.017)	0.989	1.388 (0.340–5.664)	0.648
Cavitation					
Absence (ref.) vs. presence	273 (86.1)/69 (13.9)	1.942 (1.209–3.120)	0.006	2.007 (1.163–3.463)	0.012
Air bronchogram					
Presence (ref.) vs. absence	85 (26.8)/232 (73.2)	3.174 (1.735–5.805)	< 0.001	2.805 (1.394–5.646)	0.004
Bubblelike lucency					
Absence (ref.) vs. presence	163 (51.4)/154 (48.6)	0.949 (0.641–1.406)	0.795	0.894 (0.561–1.425)	0.637
Lymphadenopathy					
Absence (ref.) vs. presence	239 (75.4)/78 (24.6)	3.304 (2.224–4.909)	< 0.001	3.213 (2.013–5.129)	< 0.001
Emphysema					
Absence (ref.) vs. presence	268 (84.5)/49 (15.5)	3.037 (1.970–4.683)	< 0.001	2.816 (1.702–4.658)	< 0.001
Pleural effusion					
Absence (ref.) vs. presence	295 (93.1)/22 (6.9)	2.514 (1.402–4.507)	0.002	2.946 (1.548–5.606)	0.001
UIP pattern					
Absence (ref.) vs. presence	300 (94.6)/17 (5.4)	2.924 (1.559–5.482)	0.001	3.227 (1.602–6.500)	0.001
Lesion in non-tumor lobe					
Absence (ref.) vs. presence	277 (87.4)/40 (12.6)	1.816 (1.102–2.994)	0.019	2.172 (1.245–3.791)	0.006
Obstructive pneumonia					
Absence (ref.) vs. presence	280 (88.3)/37 (11.7)	1.730 (1.026–2.916)	0.040	1.868 (1.023–3.409)	0.042

UIP = usual interstitial pneumonia

https://doi.org/10.3348/kjr.2020.0454

Table 3. The Multivariable Cox Regression Analysis of CT Imaging Features Predicting the Prognosis in 317 IMA Patients

CT Imaging Features	DFS		OS	
	HR (95% CI)	*P*	HR (95% CI)	*P*
Imaging subtype (solitary-type as ref.)	2.344 (1.131–4.857)	0.002		
Location (peripheral as ref.)	-	-	1.926 (1.070–3.467)	0.029
Spiculation (absence as ref.)		< 0.001		
Few (≤ 4)	1.206 (0.665–2.188)	0.537	-	-
Much (> 4)	2.405 (1.425–4.060)	< 0.001	-	-
Air bronchogram (presence as ref.)	3.300 (1.725–6.313)	< 0.001	1.895 (1.161–3.092)	0.011
Tumor density (sub-solid as ref.)	1.790 (1.167–2.745)	0.008	-	-
Emphysema (absence as ref.)	2.042 (1.205–3.461)	< 0.001	-	-
Overall stage (I as ref.)		< 0.001		< 0.001
II	3.422 (2.007–5.832)	< 0.001	4.212 (2.170–8.177)	< 0.001
III	5.096 (2.844–9.132)	< 0.001	5.947 (2.977–11.881)	< 0.001
Tumor size	-	-	1.102 (1.016–1.194)	0.019

survival; except for tumors with a mixed consolidation and GGO component, which was the only significant prognostic indicator for longer DFS (adjusted $p = 0.012$).

DISCUSSION

IMA is characterized by a distinct pathologic heterogeneity that drives unique clinical and radiologic behaviors (21). Imaging is recognized as a valuable tool providing prognostic information (8, 22). Our study demonstrated that 15 included CT imaging features correlated with the survival outcome of IMA; five among them, including imaging subtype, location, spiculation, air bronchogram, and tumor texture, persisted on multivariate analysis as independent prognostic factors. Moreover, the comparative survival analyses indicated that patients with pneumonic-type IMA had a significantly worse prognosis than those with solitary-type IMAs. The subgroup analysis further resulted in completely different prognostic factors for these two imaging subtypes.

Since IMA was proposed as a separate subtype of lung ADC in the histologic classification system in 2011, existing literature on the prognosis of IMA compared with that of other invasive ADCs differ (9, 23-25). However, the vast majority of studies suggest that IMAs have a moderate prognosis, which is better than acinar predominant subtype but worse than micropapillary/solid predominant subtype. In our results, the 5-year DFS and OS rates of IMA are 68.5% and 77.6%, respectively, which are consistent with previous works (10, 21). Regarding further survival stratification, Lee et al. (9) demonstrated that the tumor size was a significant independent poor prognostic factor; Luo et al. (23) reposted that VPI was another independent risk factor; lymph-node metastasis was also associated with worse prognosis of IMA (26). Our results are consistent with those of these studies. Moreover, we demonstrate that TNM staging was also a suitable predictor for IMA. Prior studies mainly focused on the prognostic influence of clinicopathologic information with small samples, and the imaging biomarker has not been precisely elucidated.

Based on the imaging subtype, Shimizu et al. (11) divided 29 IMAs into three types and demonstrated that the pneumonic-type correlated with a poorer prognosis compared with the solid or bubbling type. The survival comparison between solitary- and pneumonic-type IMA resulted in a similar trend in two studies with 26 and 68 cases, respectively (10, 14). However, Lee et al. (9) analyzed the DFS and OS rates of 62 nodular tumors and 19 consolidative tumors, showing no statistically significant differences ($p = 0.062$ and $p = 0.109$, respectively). The differing results may be due to varying study sample sizes and differences in definitions of CT features. Our study confirmed the prognostic impact of imaging subtypes with 317 cases. Additionally, a propensity matching to avoid the influence of clinicopathologic predictors showed that pneumonic-type IMA had a significantly worse survival compared to solitary-type IMA. These findings emphasize the distinct imaging heterogeneity of this disease and prove their prognostic ability in clinical management.

Considering the completely different presentation of solitary-type and pneumonic-type IMAs on CT, we further investigated the prognostic influence of other detailed radiologic features based on each imaging subtype. There was no significant clinicopathologic prognosticator for

https://doi.org/10.3348/kjr.2020.0454

Korean Journal of Radiology
KJR

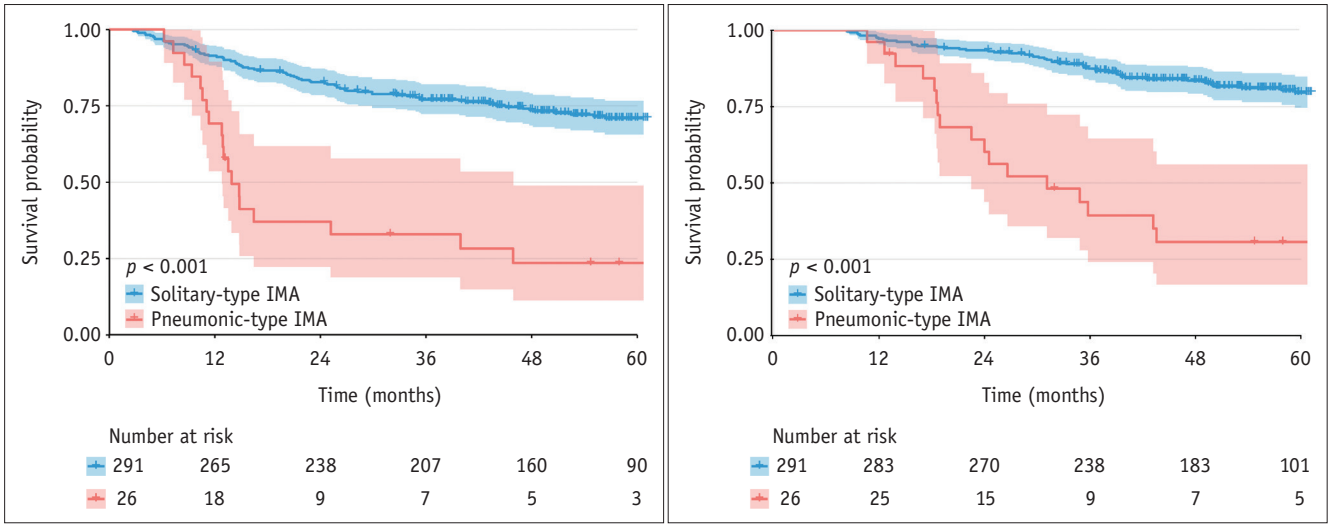

A

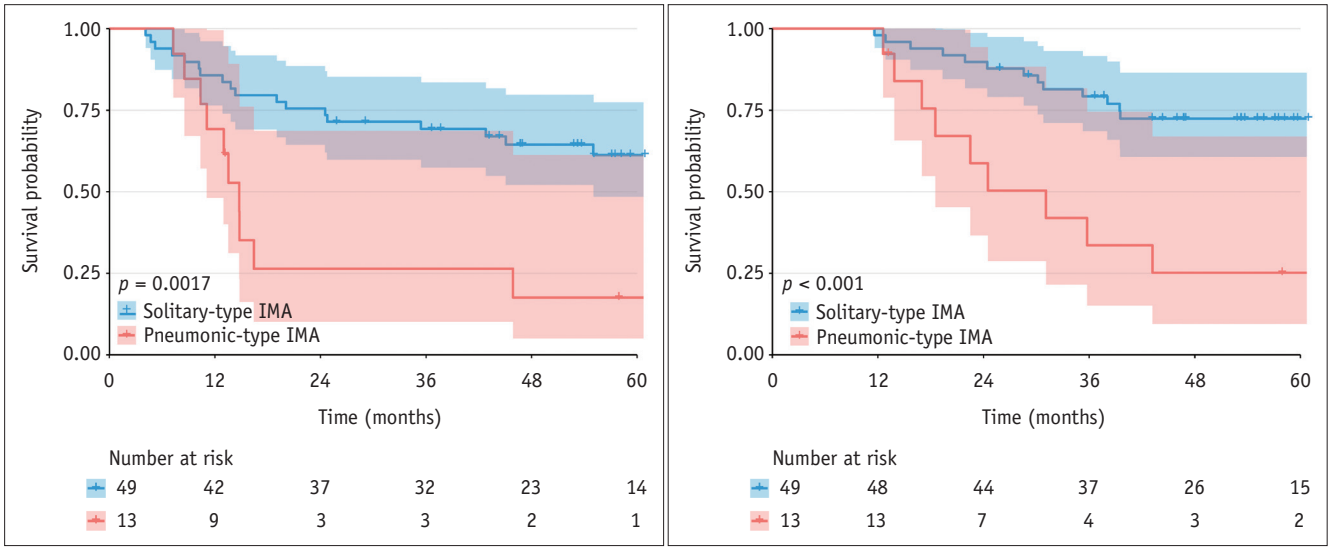

B

Fig. 3. Kaplan-Meier curves of DFS and OS according to different imaging subtypes of patients with lung IMA based on the original and propensity score-matching cohorts.
A. Original cohort. **B.** Propensity score-matching cohort. Left panel: DFS; right panel: OS. The dashed lines represent the 95% confidence interval for each curve.

pneumonic-type IMA, even the recognized TNM staging, which might be due to the small sample size of this specific imaging subtype. Interestingly, we found that pneumonic-type IMA with mixed consolidation and GGO could have a longer survival time compared with those manifesting with pure solid images. Several studies (13, 14, 27) have suggested that CT attenuation of mixed GGO and consolidation is a distinct feature of pneumonic-type IMA, which is pathologically consistent and include a mixture of mucin accumulation and invasive tumor lesions. However, the prognostic impact of this CT imaging feature, tumors with mixed consolidation and GGO may be influenced by the low incidence of pneumonic-type IMA, and need further external validation in larger datasets.

In all patients with IMAs, two other CT features describing the surrounding tissue of the tumor, air bronchogram and spiculation, were associated with increased HR for tumor recurrence or death. For IMA, the air bronchogram sign has been reported to be caused by mucus secretions with extensive alveolar filling that provide a contrasting background against which air-filled bronchi stand out (28). Miyamoto et al. (13) explained that these malignant signs of IMA, such as the spiculation, corresponded pathologically to tumor infiltration, invasion, and desmoplastic reaction

 https://doi.org/10.3348/kjr.2020.0454

Table 4. The Univariable and Multivariable Analysis of Prognostic Factors in Solitary-Type IMA Patients

Prognostic Factors	DFS			OS		
	Univariable	Multivariable Analysis		Univariable	Multivariable	
	P (Adjusted)	HR (95% CI [Adjusted])	*P* (Adjusted)	*P* (Adjusted)	HR (95% CI [Adjusted])	*P* (Adjusted)
Clinicopathologic features						
Sex (male)	0.182			0.052		
Overall stage (I as ref.)	< 0.001		< 0.001	< 0.001		< 0.001
II	< 0.001	2.335 (1.088–5.011)	0.026	< 0.001	3.494 (1.354–9.017)	0.006
III	< 0.001	5.284 (2.518–11.089)	< 0.001	< 0.001	7.857 (3.364–18.323)	< 0.001
VPI (presence)	0.016			0.018		
Tumor size	< 0.001			< 0.001		
CT imaging features						
Location (central)	0.112			0.050	1.921 (0.799–4.617)	0.190
Spiculation (absence as ref.)	< 0.001		0.068	0.006		
Few (≤ 4)	1.000	0.953 (0.454–2.000)	1.000	0.990		
Much (> 4)	< 0.001	1.855 (0.943–3.651)	0.082	0.016		
Pleural retraction (presence)	0.026	1.622 (0.921–2.857)	0.112	0.256		
Tumor density (pure-solid)	0.002			0.024		
Air bronchogram (absence)	< 0.001	3.731 (1.596–8.721)	0.002	0.008	4.264 (1.618–11.239)	0.002
Lymphadenopathy (presence)	< 0.001			< 0.001		
Emphysema (presence)	< 0.001	1.273 (1.124–4.370)	0.024	0.002	1.315 (1.016–1.701)	0.034
Pleural effusion (presence)	0.034			0.042		
UIP pattern (presence)	0.002			0.002		
Lesion in non-tumor lobe (presence)	0.032			0.012		

and concurrently expanded the tumor cell proliferation along the surrounding alveolar walls. Our study advocated that these CT features suggestive of macroscopic tumor spread were useful imaging prognosticators in IMA.

There are several limitations in this study. First, the retrospective design of the study may cause an inevitable selection bias. Second, all included CT features were interpreted subjectively by three professional thoracic radiologists, which may cause variability in routine clinical application. Nevertheless, we have confirmed that these imaging findings from different readers have good agreements. Third, although we tried to include all available consecutive IMA patients by a logical selection process, the low incidence of pneumonic-type IMA may influence the generalizability of our results. Additional larger and balanced validation studies are warranted in the future.

An accurate knowledge of cancer patients' prognosis is a valuable tool in clinical management, particularly in a non-invasive way. In this study, we demonstrated that CT imaging features of IMA could be non-invasive image biomarkers for survival prediction. These findings may enrich the radiologist's knowledge of this specific population, provide implications for further risk stratification, and lead to appropriate therapeutic strategies for patients with IMA.

Supplementary Materials

The Data Supplement is available with this article at https://doi.org/10.3348/kjr.2020.0454.

Conflicts of Interest

The authors have no potential conflicts of interest to disclose.

Acknowledgments

The authors wish to thank the biostatistician, Prof. Zhang Aihong (Department of Medical Statistics, Tongji University School of Medicine, Shanghai, China), for the design and guidance of statistical analysis in this study.

ORCID iDs

Tingting Wang
https://orcid.org/0000-0002-3682-3039

Korean Journal of Radiology
KJR

Chang Chen
https://orcid.org/0000-0003-2841-1250

REFERENCES

1. Siegel RL, Miller KD, Jemal A. Cancer statistics, 2019. *CA Cancer J Clin* 2019;69:7-34
2. Bray F, Ferlay J, Soerjomataram I, Siegel RL, Torre LA, Jemal A. Global cancer statistics 2018: GLOBOCAN estimates of incidence and mortality worldwide for 36 cancers in 185 countries. *CA Cancer J Clin* 2018;68:394-424
3. Lee HY, Lee SW, Lee KS, Jeong JY, Choi JY, Kwon OJ, et al. Role of CT and PET imaging in predicting tumor recurrence and survival in patients with lung adenocarcinoma: a comparison with the International Association for the Study of Lung Cancer/American Thoracic Society/European Respiratory Society Classification of Lung Adenocarcinoma. *J Thorac Oncol* 2015;10:1785-1794
4. Fan L, Fang M, Li Z, Tu W, Wang S, Chen W, et al. Radiomics signature: a biomarker for the preoperative discrimination of lung invasive adenocarcinoma manifesting as a ground-glass nodule. *Eur Radiol* 2019;29:889-897
5. Travis WD, Brambilla E, Noguchi M, Nicholson AG, Geisinger KR, Yatabe Y, et al. International Association for the Study of Lung Cancer/American Thoracic Society/European Respiratory Society International Multidisciplinary Classification of Lung Adenocarcinoma. *J Thorac Oncol* 2011;6:244-285
6. Shim HS, Kenudson M, Zheng Z, Liebers M, Cha YJ, Hoang Ho Q, et al. Unique genetic and survival characteristics of invasive mucinous adenocarcinoma of the lung. *J Thorac Oncol* 2015;10:1156-1162
7. Geles A, Gruber-Moesenbacher U, Quehenberger F, Manzl C, Al Effah M, Grygar E, et al. Pulmonary mucinous adenocarcinomas: architectural patterns in correlation with genetic changes, prognosis and survival. *Virchows Arch* 2015;467:675-686
8. Austin JH, Garg K, Aberle D, Yankelevitz D, Kuriyama K, Lee HJ, et al. Radiologic implications of the 2011 classification of adenocarcinoma of the lung. *Radiology* 2013;266:62-71
9. Lee HY, Cha MJ, Lee KS, Lee HY, Kwon OJ, Choi JY, et al. Prognosis in resected invasive mucinous adenocarcinomas of the lung: related factors and comparison with resected nonmucinous adenocarcinomas. *J Thorac Oncol* 2016;11:1064-1073
10. Nie K, Nie W, Zhang YX, Yu H. Comparing clinicopathological features and prognosis of primary pulmonary invasive mucinous adenocarcinoma based on computed tomography findings. *Cancer Imaging* 2019;19:47
11. Shimizu K, Okita R, Saisho S, Maeda A, Nojima Y, Nakata M. Clinicopathological and immunohistochemical features of lung invasive mucinous adenocarcinoma based on computed tomography findings. *Onco Targets Ther* 2017;10:153-163
12. Limkin EJ, Sun R, Dercle L, Zacharaki EI, Robert C, Reuzé S, et al. Promises and challenges for the implementation of computational medical imaging (radiomics) in oncology. *Ann Oncol* 2017;28:1191-1206
13. Miyamoto A, Kurosaki A, Fujii T, Kishi K, Homma S. HRCT features of surgically resected invasive mucinous adenocarcinoma associated with interstitial pneumonia. *Respirology* 2017;22:735-743
14. Watanabe H, Saito H, Yokose T, Sakuma Y, Murakami S, Kondo T, et al. Relation between thin-section computed tomography and clinical findings of mucinous adenocarcinoma. *Ann Thorac Surg* 2015;99:975-981
15. Lee HY, Lee KS, Han J, Kim BT, Cho YS, Shim YM, et al. Mucinous versus nonmucinous solitary pulmonary nodular bronchioloalveolar carcinoma: CT and FDG PET findings and pathologic comparisons. *Lung Cancer* 2009;65:170-175
16. Hsu CP, Chen CY, Hsu NY. Bronchioloalveolar carcinoma. *J Thorac Cardiovasc Surg* 1995;110:374-381
17. Travis WD, Brambilla E, Nicholson AG, Yatabe Y, Austin JHM, Beasley MB, et al. The 2015 World Health Organization classification of lung tumors: impact of genetic, clinical and radiologic advances since the 2004 classification. *J Thorac Oncol* 2015;10:1243-1260
18. Goldstraw P, Chansky K, Crowley J, Rami-Porta R, Asamura H, Eberhardt WE, et al. The IASLC lung cancer staging project: proposals for revision of the TNM stage groupings in the forthcoming (eighth) edition of the TNM classification for lung cancer. *J Thorac Oncol* 2016;11:39-51
19. Liu Y, Kim J, Qu F, Liu S, Wang H, Balagurunathan Y, et al. CT features associated with epidermal growth factor receptor mutation status in patients with lung adenocarcinoma. *Radiology* 2016;280:271-280
20. Bland JM, Altman DG. Multiple significance tests: the bonferroni method. *BMJ* 1995;310:170
21. Boland JM, Maleszewski JJ, Wampfler JA, Voss JS, Kipp BR, Yang P, et al. Pulmonary invasive mucinous adenocarcinoma and mixed invasive mucinous/nonmucinous adenocarcinoma-a clinicopathological and molecular genetic study with survival analysis. *Hum Pathol* 2018;71:8-19
22. Detterbeck FC, Franklin WA, Nicholson AG, Girard N, Arenberg DA, Travis WD, et al. The IASLC lung cancer staging project: background data and proposed criteria to distinguish separate primary lung cancers from metastatic foci in patients with two lung tumors in the forthcoming eighth edition of the TNM classification for lung cancer. *J Thorac Oncol* 2016;11:651-665
23. Luo J, Wang R, Han B, Zhang J, Zhao H, Fang W, et al. Analysis of the clinicopathologic characteristics and prognostic of stage I invasive mucinous adenocarcinoma. *J Cancer Res Clin Oncol* 2016;142:1837-1845
24. Yoshizawa A, Sumiyoshi S, Sonobe M, Kobayashi M, Fujimoto M, Kawakami F, et al. Validation of the IASLC/ATS/ERS lung adenocarcinoma classification for prognosis and association with EGFR and KRAS gene mutations: analysis of 440 Japanese patients. *J Thorac Oncol* 2013;8:52-61
25. Yoshizawa A, Motoi N, Riely GJ, Sima CS, Gerald WL, Kris MG,

 https://doi.org/10.3348/kjr.2020.0454

et al. Impact of proposed IASLC/ATS/ERS classification of lung adenocarcinoma: prognostic subgroups and implications for further revision of staging based on analysis of 514 stage I cases. *Mod Pathol* 2011;24:653-664
26. Cai D, Li H, Wang R, Li Y, Pan Y, Hu H, et al. Comparison of clinical features, molecular alterations, and prognosis in morphological subgroups of lung invasive mucinous adenocarcinoma. *Onco Targets Ther* 2014;7:2127-2132
27. Akira M, Atagi S, Kawahara M, Iuchi K, Johkoh T. High-resolution CT findings of diffuse bronchioloalveolar carcinoma in 38 patients. *AJR Am J Roentgenol* 1999;173:1623-1629
28. Wong JS, Weisbrod GL, Chamberlain D, Herman SJ. Bronchioloalveolar carcinoma and the air bronchogram sign: a new pathologic explanation. *J Thorac Imaging* 1994;9:141-144

https://doi.org/10.3348/kjr.2020.0454